Article

The Expected Shoreline Effect of a Marine Energy Farm Operating Close to Sardinia Island

Florin Onea and Eugen Rusu*

Department of Mechanical Engineering, Faculty of Engineering, Dunarea de Jos University of Galati, 47 Domneasca Street, 800008 Galati, Romania; floryn.onea@gmail.com
* Correspondence: eugen.rusu@ugal.ro; Tel.: +40-740-205-534

Abstract: Coastal areas are defined by numerous opportunities and threats. Among them we can mention emerging renewable projects and on the other hand coastal erosion. In the present work, the impact of a generic wind–wave farm on the nearshore waves and currents in the vicinity of the Porto Ferro inlet (northwest Sardinia) was assessed. Using a reanalysis wave dataset that covers a 40-year interval (1979–2018), the most relevant wave characteristics in the target area were identified. These can reach during winter a maximum value of 7.35 m for the significant wave height. As a next step, considering a modeling system that combines a wave model (simulating waves nearshore (SWAN)) and a surf model, the coastal impact of some generic marine energy farms defined by a transmission coefficient of 25% was assessed. According to the results corresponding to the reference sites and lines defined close to the shore, it becomes obvious that there is a clear attenuation in terms of significant wave heights, and as regards current velocities, although the general tendency for them to decrease, there are, however, some situations when the values of the nearshore current velocities can also decrease. Finally, we can mention that the presence of a marine energy farm seems to be beneficial for the beach stability in this particular coastal environment, and in some cases the transformation of the breaking waves from plunging to spilling is noticed.

Keywords: Sardinia; coastal protection; wind–wave projects; nearshore variations; longshore currents

1. Introduction

Marine regions represent suitable environments for development of marine energy farms, the most promising concepts being associated with wind and wave energy extraction. Since there is a strong connection between the two resources, and the offshore wind sector is a mature market, especially in Europe, co-locating wave farms together with existing wind projects represents a viable approach. This is because in such a way, it is possible to reduce the initial costs associated with a wave project and also to increase the amount of electricity output [1–3]. In addition, for the wind farms located close to the shoreline, such an approach can provide also in certain cases effective coastal protection by reducing the power of the waves propagating towards the shores [4–8].

However, enclosed seas are defined by different marine conditions, in which it is possible to encounter high winds suitable for electricity production, but relatively smaller waves due to the limited fetch. This is also the case of the Mediterranean Sea, which includes numerous islands that represent wave energy hot spots (for example Sardinia or Crete islands), where the waves are sometimes higher than those close to the European continental coastlines [9–11]. In the works of Franzitta and Curto and in Liberti et al. [12,13] such analyses were performed considering the renewable energy potential of some islands in the Mediterranean Sea. There is an obvious interest in the wind and wave conditions in this area, and as a consequence various wave atlases were

designed. Some examples are the works of Ayat [14], Cavaleri [15], and Soukissian et al. [16]. In terms of wind and waves, more significant resources are noticed in the western part of the basin, especially in the area between Sardinia and France. An average wind speed (at 10 m height) of 8 m/s is normal in this area, while the average value of significant wave heights is about 1.4 m, according to the ERA-interim data. ERA stands for 'ECMWF Re-Analysis', where ECMWF indicates the European Centre for Medium-Range Weather Forecasts. In Onea et al. [17] the regional wind conditions were compared with similar ones from the vicinity of some operational offshore wind farms (located in the UK), the conclusion being that during the interval February–August (seven months), similar performances were noticed. The island of Crete (north of Sardinia) was also considered for investigation; Lavidas and Venugopal [18] proposed the combined use of wind and wave power in order to support the electricity grid of this island. According to this study, the best performances of a co-located wave–wind project were expected for the interval from January until May, and representative values in August were also noticeable. In Vannucchi and Cappietti [19], a complete assessment of the wave conditions was carried out in order to identify the most relevant hotspots in terms of electricity production. According to these results, the most suitable sites are Sardinia and Sicily where the wave energy can reach average values of 11.4 kW/m. It must also be highlighted that the work of Iuppa et al. [20] mentions that the western part of Sicily presents more significant wave conditions that can frequently exceed 8 kW/m. Wave energy is an emerging sector, and it is expected that some other semi-enclosed basins will become attractive in the near future, as in the case of the Persian Gulf [21].

As it is well known, shoreline erosion is a natural process that affects all the coastlines. Furthermore, some previous studies suggest that almost 40% of the beaches in the Mediterranean Sea (European side) are affected by these events, and since 1960 almost three-quarters of the sand dunes located between Spain and Sicily have disappeared. The erosion processes are more severe in the Adriatic Sea (25.6%), followed by the Ionian Sea (22.5%), Balearic Islands (19.6%), and Sardinia (18.4%) [22]. The local authorities take very seriously the problem of beach stability, it being strictly forbidden for the tourists to take as souvenirs sand, stones, or seashells. Even in these conditions, it was estimated that on the Elmas airport (Sardinia) almost five tons of sand were seized in just three summer months in 2015 [23]. In general, there are little options to tackle the beach erosion, most of the existing literature being related to observations of these events as in the case of Sardinia [24], Maresme coast [25], or Menorca Island [26], respectively. More than this, it is expected that as a consequence of global warming, the erosion risk will increase by 13% across this region by 2100. Thus, it is estimated also that almost 42 UNESCO (United Nations Educational, Scientific and Cultural Organization) World Heritage sites are already affected by coastal erosion [27]. Furthermore, the islands' environments are more vulnerable to the impact of the sea-level variations, this issue being already highlighted for the Aegean archipelago [28].

In a first approach, a viable direction to develop wave projects is represented by collocation. This is to deploy wave energy converters in places where offshore wind turbines already operate. The idea of collocation is related mainly to the enhancement of the efficiency of the wave energy converters, since in this way they would benefit from the existing infrastructure of the wind turbines. In this way the wave energy price would become more attractive (see for example Ciortan et al. [29]).

By looking at most of the studies focused on the wave energy potential in the Mediterranean Sea, we notice that they can be structured in two parts: a) assessment of the resources; and b) evaluation of the performances corresponding to some wave energy converters. Since at this moment, the idea of using a wave farm to protect a particular beach sector from this region is not taken into account, we consider that this is the gap covered by the present work

In this context, the objective of the present work is to highlight the possible benefits coming from the implementation of a generic (wind/wave) marine energy farm in the western part of Sardinia Island, by focusing on three main directions:

Establish the most relevant sea state conditions that define this coastal environment;

Evaluate the impact of a marine energy project on the local wave conditions;

Assess the variations of the nearshore currents in the presence of a generic marine energy farm.

2. Materials and Methods

2.1. Study Area: Sardinia

Located in the northwestern part of the Mediterranean Sea, Sardinia is one of the largest islands in this region with a total surface of 24,000 km², being located at approximately 180 km from the mainland (Figure 1). This island is well known for wind energy potential, being also noticed consistent solar radiations that can be easily used to cover the energy demand for the almost 1,600,000 people living in this area [30]. The tide does not exceed 30 cm, while the dominant wind is the Mistral that blows over numerous bays defined by white sand and gravelly pocket beaches [31]. Most of the sediments are associated with bioclastic sand that is produced by sea-grass meadows, while the waves feed the beaches with sand and pebbles coming from erosion of the bay–cliff regions. The beaches from the northwest of the island are defined by medium sand with geometric sizes in the range of 291–384 μm [31]. The study area targeted in the present work is located near Porto Ferro beach. This is well known for the touristic activities, especially due to the high quality of its bathing areas. As a general feature, this natural inlet is defined by a total length of 2 km, being flanked on the south by twenty-meter high dunes that separate it from the Largo Baratz [32].

2.2. ERA-Interim Wave Data

The scenarios considered for investigations are designed based on the ERA-interim dataset, which is a product of the European Center for Medium-Range Weather Forecasts [33]. The accuracy of this reanalysis dataset in the target area was already discussed in Vicinanza et al. [34] that assessed the wave energy potential in the north-western part of Sardinia for the 20-year interval (January 1989 to December 2009). From the comparison with in situ wave measurements coming from the Alghero buoy (close to Porto Ferro), it was found that there are some differences between the two datasets. Thus, it was noticed a tendency for the ECMWF data to slightly underestimate especially the higher energy conditions.. At this point, it is important to mention that almost 9% of missing data correspond to the Alghero observations; these gaps being considered as calm conditions.
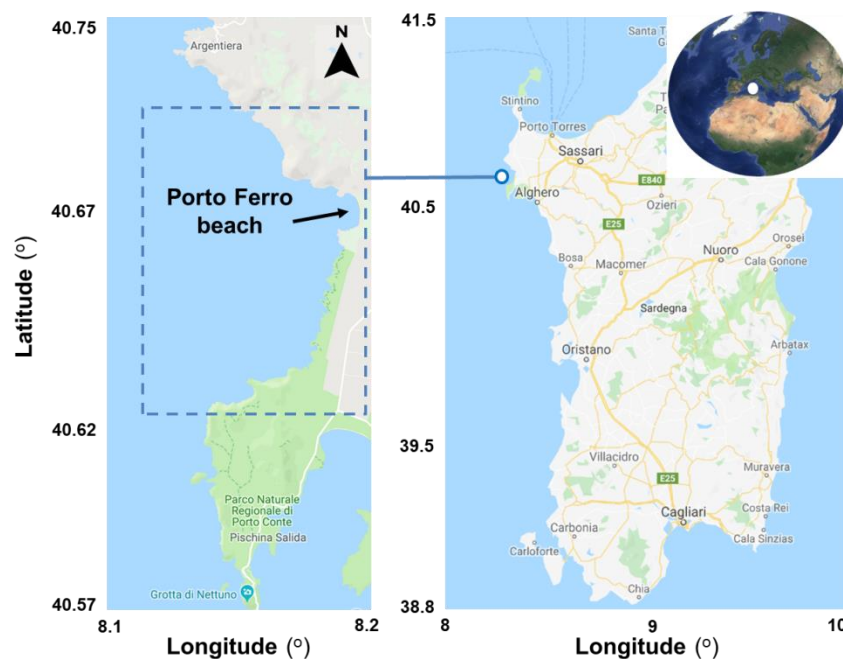
Figure 1. Sardinia Island and the geographical location of the target area. Figure processed from Google Earth (2019).

In the present work, three wave parameters were considered for assessment. These are: a) significant wave height—*Hs* (m), b) mean wave period—*Tm* (s), and c) mean wave direction—*Dir* (°), waves coming from the North (0°). A total of 40-years of data (January 1979–December 2018) was considered. The data were defined by a time step of 6h and a spatial resolution of 0.25° × 0.25°.

2.3. The ISSM Model System and the Case Sudies

The ISSM (interface for simulating waves nearshore (SWAN) and surf models) [35,36] computational tool was used to assess the impact of the generic marine energy farm on the local wave conditions and on the shoreline processes. This ISSM modeling system has been intensively validated in the target area against measurements provided by an ADCP (acoustic Doppler current profiler) for the nearshore level and by Nortek vectors in the surf zone areas. The results were presented in Rusu and Soares [37] and Goncalves et al. [38], respectively. High quality bathymetry resulted from merging various techniques [37]. Thus, the coast and the land topography were generated using a global positioning system receiver. For depths between 2 and 10 meters, corresponding to shallow water, high resolution bathymetric data was provided by an echo sounder and a GPS receiver mounted on a boat. Finally, a vessel based multibeam system provided the deeper water (12–50) m bathymetry. All these data were merged and transformed in a rectangular grid via the bathymetric module of the ISSM system [35].

The wave component of this system consisted of the SWAN (simulating waves nearshore) model, which is a spectral phase averaged model capable of evaluating the wave transformation in coastal areas based on the wave action balance equation that includes sources and sinks defining the evolution of the wave spectrum in spectral, time, and geographical spaces [39]:

$$\frac{\partial N}{\partial t} + \nabla\left[(\vec{c}_g + \vec{V})N\right] + \frac{\partial}{\partial \sigma}c_\sigma N + \frac{\partial}{\partial \theta}c_\theta N = \frac{S}{\sigma} \tag{1}$$

where N is the action density spectrum, σ is the relative frequency, θ is the wave direction, and $\vec{V}$ represents the velocity of the ambient current, which is considered uniform. The propagation velocities of the wave energy are: the relative group velocity $\vec{c}_g$ in the physical space $\left(\vec{c}_g = \partial\sigma/\partial\vec{k}\right)$ and the propagation velocities in the spectral space $c_\sigma = \dot{\sigma}$ and $c_\theta = \dot{\theta}$. S represents the source and sink terms.

As a next step, the SWAN outputs were used as input for the surf of Navy standard surf model [35]. These wave model outputs used as input for the surf model were significant wave height (*Hs*), mean wave period (*Tm*), and mean wave direction (*DIR*) [37]. The wave period and direction were entered as direct input, while as regarding the wave height, since the root mean square wave height (*Hrms*) was required in the nearshore circulation model, this was derived from the significant wave height (*Hrms* = 0.707 *Hs*). Furthermore, the bathymetry in 100 points equally distanced along the reference line selected graphically directly from the SWAN computational domain was also interpolated directed from the SWAN model. The Navy standard surf model assesses the longshore current variations along cross shore profiles with the following relation [40]:

$$\tau_y^r + \rho\frac{\partial}{\partial x}\left[\mu h\frac{\partial V}{\partial x}\right] - \left\langle\tau_y^b\right\rangle + \left\langle\tau_y^w\right\rangle = 0 \tag{2}$$

where τ_y^r, is the longshore directed radiation stress due to the incident waves, the second term represents the horizontal mixing term due to cross-shore gradients in the longshore current velocity *V*, the third term, τ_y^b, is the wave averaged bottom stress, and the last term, τ_y^w, represents the long-shore wind stress.

In Figure 2 is presented the SWAN computational domain that includes the bathymetric map and the four scenarios (CS1, CS2, CS3, and CS4) considered for evaluation. The scenarios were built by taking as a core the structure of an offshore wind farm, more precisely the Kentish Flats project, which includes thirty Vestas V90-3.0 generators. The distance between the turbines in the gird is close to 0.7 km (along x and y directions), this being close to eight rotor diameters [41]. Nevertheless, for the present work only 24 systems were considered (6 × 4 turbines), in order to fit in the computational domain. Several scenarios were defined, each involving at least one generic wave farm defined by a 25% absorption characteristic. This means that 75% of the incoming waves will not be affected by these obstacles. More details about the scenarios are presented in Table 1, a similar approach being considered to simulate the impact of various wave farm configurations in this region [42].

The SWAN computational domain is defined by a rectangle rotated 11 degrees from the horizontal, having a length of 7200 m (in x-direction) and 11475 m (in y-direction). The spatial resolution of the computational grid is 25 m in both directions. In the spectral space, 34 frequencies and 36 directions have been defined. We used this configuration for which situation analyzed simulations in the stationary mode were performed with the wave model.
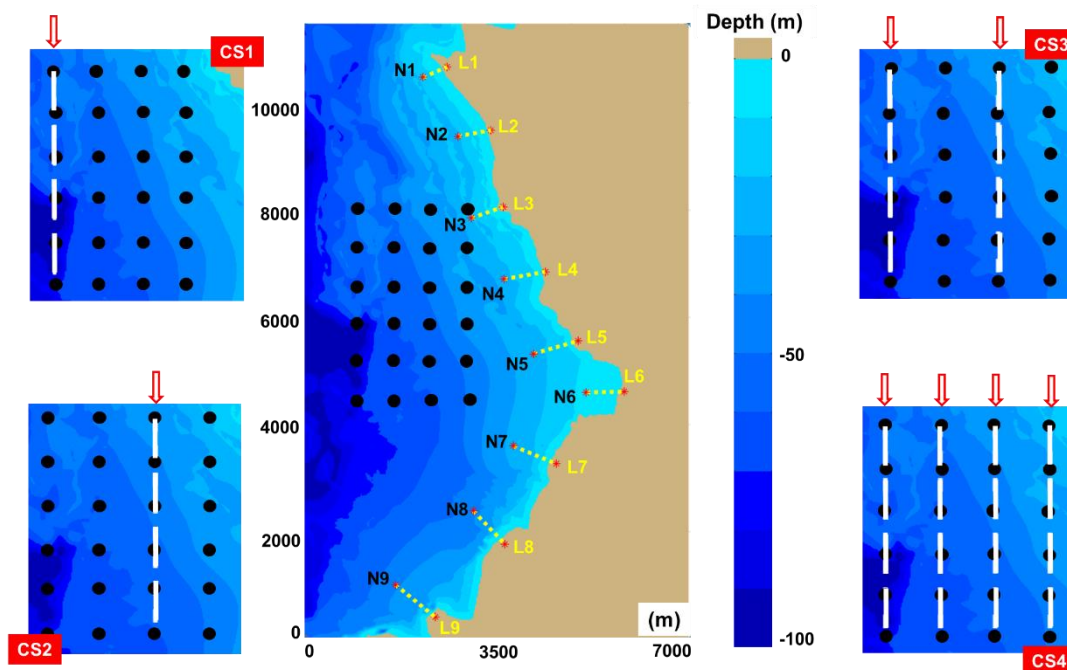

Figure 2. Computational domain of the target area (bathymetric map), including the wind farm configuration, the main scenarios (CS1, CS2, CS3 and CS4), the nearshore reference points (N1–N9), and the reference lines (L1–L9).

Table 1. Scenarios selected for the implementation in the wave modeling system.

Reference	Wave absorption	Description
No farm	No restriction	Basic scenario—no wave farm
CS1	25%	One generic marine farm—offshore area (1st column)
CS2	25%	One generic marine farm—nearshore area (3rd column)
CS3	25% (each)	Two generic marine farms—1st column and 3rd column
CS4	25% (each)	Four generic marine farms—one per column

The impact of the generic farm(s) in the geographical space were evaluated through spatial maps, while the nearshore points N1–N9 provided more accurate details regarding the nearshore wave transformation. The reference lines L1–L9 were used to estimate the variations of the

longshore currents close to the shoreline, and to identify the most relevant physical processes associated with the waves in the breaking area.

3. Results

3.1. Analysis of the Wave Data

Figure 3 presents the average *Hs* spatial distribution (average values) resulting from processing the ERA-interim data. The site O1 that was further used to identify the conditions occurring on the external boundary of the SWAN computational domain was also included. According to these data, it is clear that the western part of Sardinia presented higher wave conditions, with a maximum *Hs* average value of 1.2 m compared to values of 0.75 m that were characteristic of the eastern part. According to these results, a wave farm implemented near the Porto Ferro area may represent a win–win project, since it is expected to generate some electricity production, on one hand, and to reduce the erosion effects associated with wave action, on the other hand.
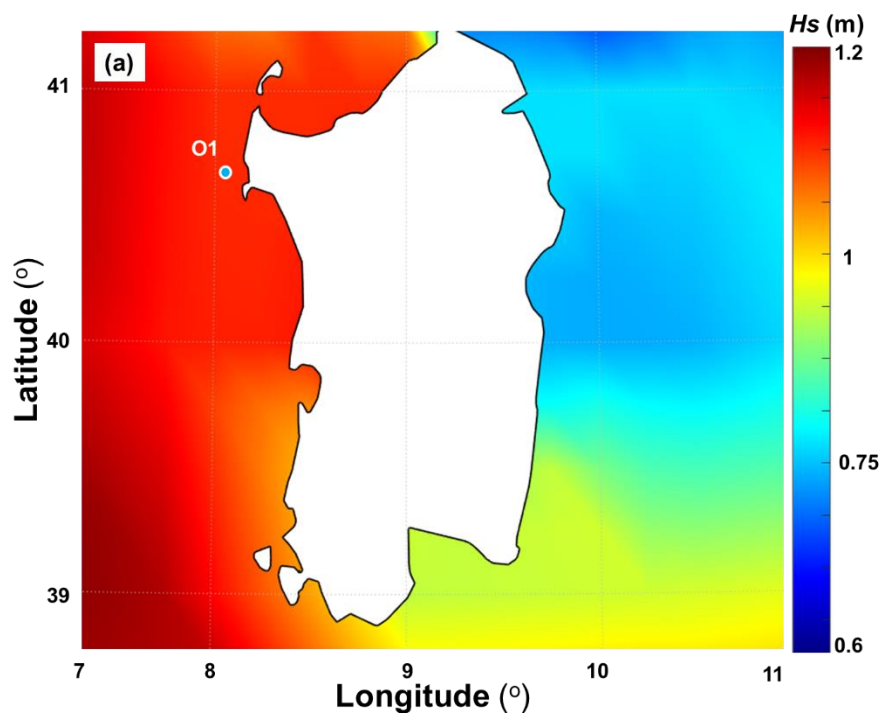

Figure 3. *Hs* spatial distribution (average values) considering the 40-year time interval (January 1979 to December 2018) of ERA-interim data. The map also indicates the position of the point O1 that is considered to assess the wave conditions in the vicinity of the simulating waves nearshore (SWAN) computational domain.

As a next step, the seasonal variations (in %) are presented in Figure 4, being defined for: a) winter (December, January, February); b) spring (March, April, May); c) summer (June, July, August); and d) autumn (September, October, November). These seasonal variations were computed as the *Hs* differences (in %) between the average values corresponding to the four main seasons and the average values corresponding to the total distribution divided by the same average values corresponding to the total distribution, considering the 40-years of ERA-interim data. This figure gives a picture of how the significant wave height was biased in each season in relation to the *Hs* mean value for the total time.
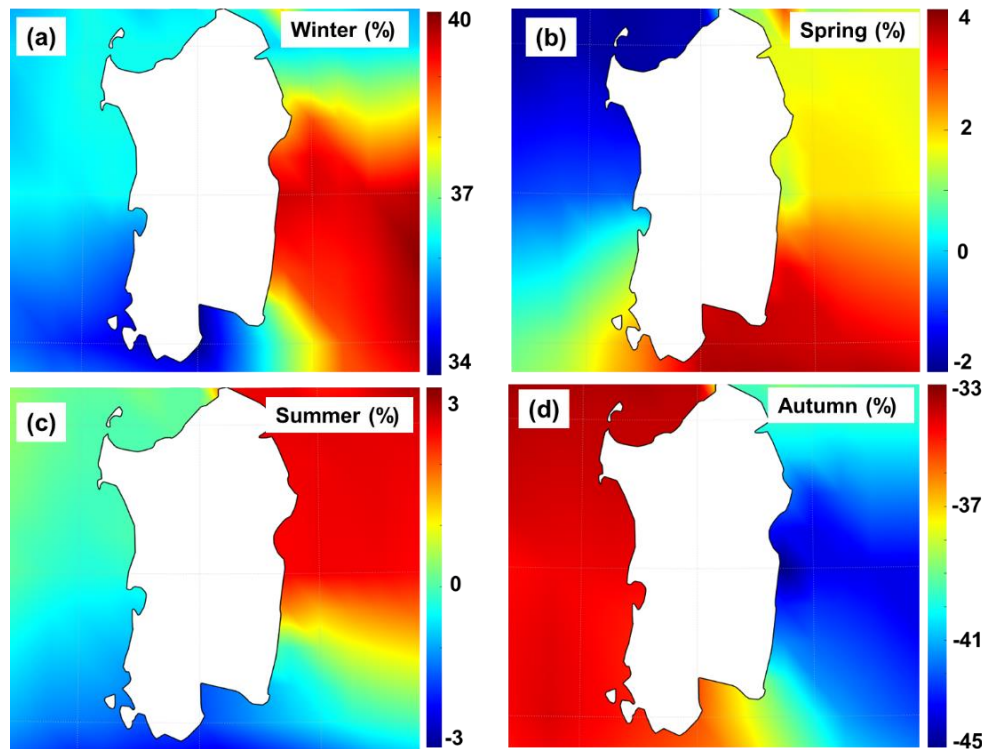
Figure 4. *Hs* differences (average values in %) between the average values corresponding to the four main seasons and average values corresponding to the total distribution divided by the same average values corresponding to the total distribution, considering the 40-years of ERA-interim data, where: (**a**) winter; (**b**) spring; (**c**) summer; (**d**) autumn.

Reporting on the total distribution, we noticed during winter an increase of the significant wave height with almost 40% for the eastern sector, while in the south–west a minimum of 34% was observed. The Porto Ferro conditions were between these two values. A mixed pattern occurred during spring, when in the north–west a decrease of almost 2% was noticed, compared to an increase of 4% in the southeast. In the central part of Sardinia, there were some areas presenting little or no fluctuations. During summer, more significant variations were noticed in the eastern side, whereas in the northeast an *Hs* increase of 3% occurred, while in the southern extremity a decrease was observed. Autumn seemed to be the least suitable season for the wave energy production, when decreases of the *Hs* values in the range of 33%–45% were noticed.

Figure 5 presents the wave conditions for the reference point O1. From the analysis of the time series, we noticed that the *Hs* values could often reach values of 6 m. In terms of percentile analysis (Figure 5b), *Hs* indicated close values during winter and autumn. Thus, a maximum value of 7.35 m was noticed. For the other two seasons (spring and summer), the Hs values were in the range of 0.84–6.17 m (spring) and 0.52–5.1 m (summer). As for the wave period, an extreme value of 11 s was expected in the winter, followed by 10.9 s in autumn, and 9.4 s in summer. A minimum wave period value of 4.3 s was expected in summer, and this value could increase up to 5.7 s in winter. From the analysis of the wave directions (Figures 5d,e), we noticed that there were no significant differences in terms of directions, both distributions (winter and summer) indicating the northwest sector (315°) as dominant. On the other hand, important differences occurred in terms of the *Hs* classes, the winter distribution indicating values higher than four meters.

Table 2 summarizes the main statistical values presented in Figure 5. As a next step, only two scenarios were considered for the SWAN simulations. These were summer (A and B) and winter (A and B).
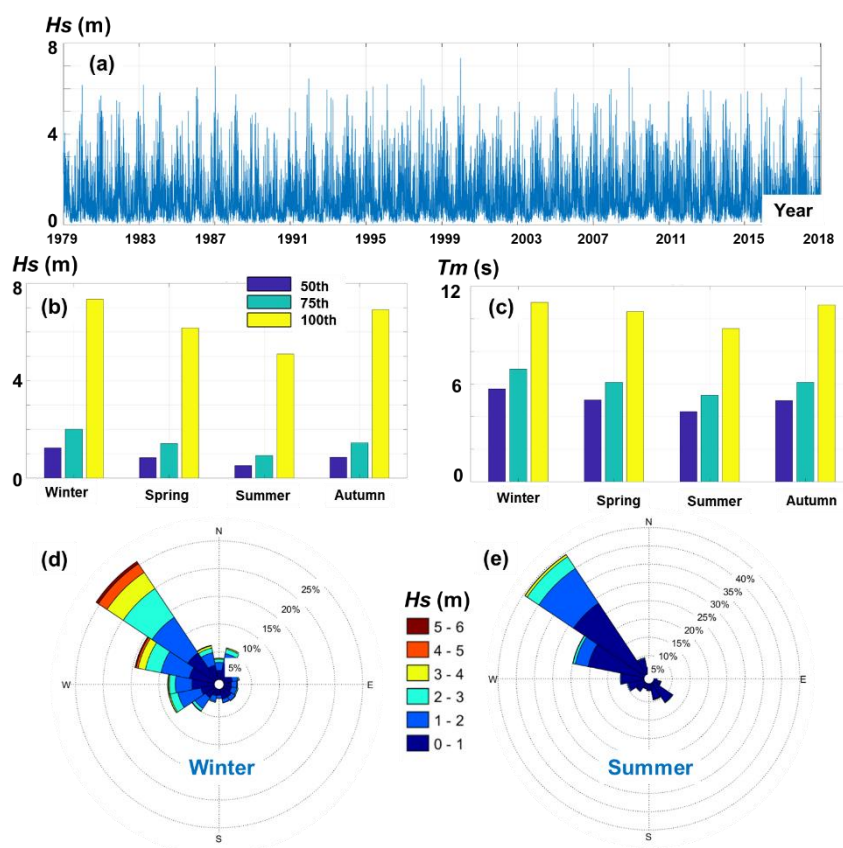
Figure 5. Wave conditions corresponding to the geographical position of the point O1, according to the ERA-interim data (January 1979 to December 2018). The results are indicated in terms of: (**a**) *Hs* time series; (**b**) and (**c**) 50, 75, and 100 percentiles of the parameters *Hs* and *Tm*, respectively, for each season; (**d**) and (**e**) wave roses computed for the winter and summer seasons, respectively.

Table 2. Statistics of the wave conditions near the site O1 according to the 40-years of European Center for Medium-Range Weather Forecasts (ECMWF) wave data (January 1979 to December 2018).

Scenarios		Wave Parameters		
		Hs (m)	*Tm* (s)	*Dir* (°)
Winter	A (75 percentile)	2.01	6.91	315
	B (100 percentile)	7.35	11	
Spring	A	1.42	6.11	315
	B	6.17	10.44	
Summer	A	0.93	5.31	315
	B	5.1	9.4	
Autumn	A	1.45	6.11	315
	B	6.91	10.84	

3.2. Coastal Impact of the Generic Farm(s)

There are various approaches considering the degree of absorption of the wave energy by a marine energy farm. This depends on the wave energy converters (WECs) considered and also on the characteristics of the incoming waves. The most important wave parameters related to the wave energy absorption are the significant wave height, wave period, and wave direction. Thus, this is a dynamic process, and the most relevant indicator related to the wave energy absorption is the capture that can be estimated with certain accuracy for each particular situation. However, in the present work a generic marine farm is considered together with some relevant scenarios defined from the analysis of the long term wave parameters in the geographical space targeted. That is why

an average absorption coefficient of 25% was considered in the present work. Several authors consider this value a realistic approach for a generic wave farm, as in the case of Rusu and Onea at 20% [4] or Onea and Rusu at 25% [42]. In the work of Stokes and Conley [43], a WEC derived absorption index was proposed that could go up to 42%.

From this perspective, a first evaluation is provided in Figure 6 for the scenario Summer A. From the spatial distribution of the wave fields (subplots 6a–e), we noticed that the impact of the generic farm was less visible for the scenario CS1 compared to CS4, where in the area between the marine farm and the coastline we noticed lower values. A more accurate evaluation was provided by the analysis performed in the N-points. Thus, in the case of the points N1, N2, and N9 no variation in the presence of the generic farm occurred. Looking at the shadowing effects, we noticed that for the scenario that involved a particular wave direction (NW) and the orientation of the WEC lines in the geographical space, little (or no) variations were expected for these sites. Therefore, these points were used as a reference in order to assess the accuracy of the results, and no variation was expected regardless of the wave conditions or scenario considered.
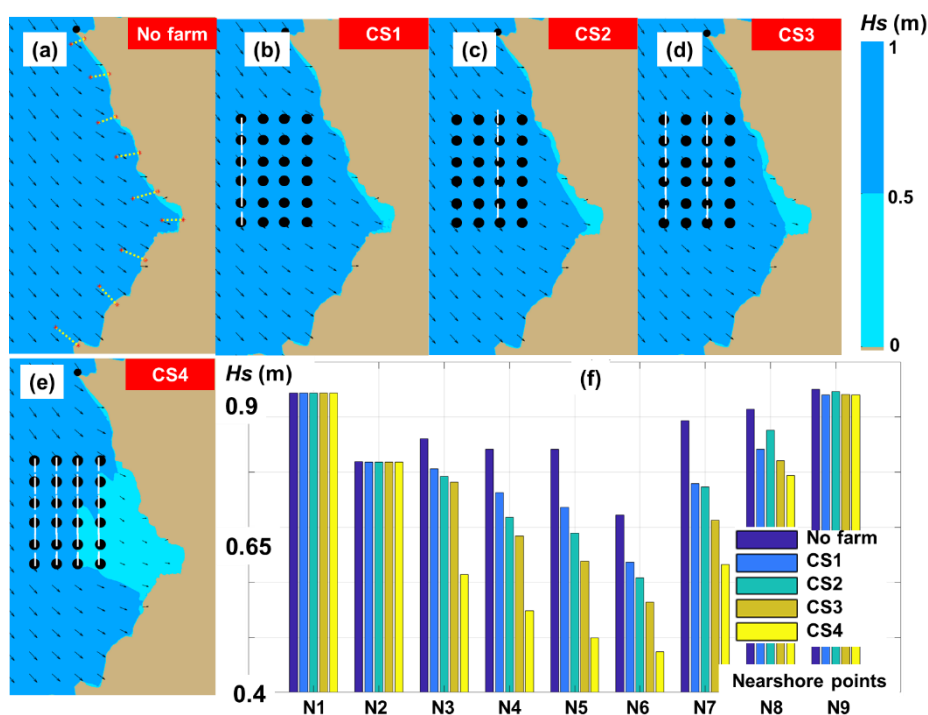

Figure 6. Influence of the generic marine farm taking into account an energetic summer event (case Summer A as defined in Table 2). The results correspond to: (**a**–**e**) *Hs* spatial variations considering various scenarios; (**f**) distribution of the *Hs* values near the nearshore points N1–N9. The arrows in the plots represent the wave direction.

By comparing the scenarios CS1 and CS2, we noticed that the impact of the wave farm was more visible for the scenario CS2, except the point N8, when a reverse pattern was noticed. In general, there were relatively small differences between the scenarios CS1, CS2 and CS3, while a significant impact is noticed for CS4, especially in the case of the reference points N3–N7. Table 3 presents the *Hs* differences (in %) between the no farm scenario and the four scenarios considered. In the case of the points N1, N2 and N9 the variation is negligible, being expected a maximum attenuation of 1.1%. The sites N4 and N5 indicate in general higher values that start from 14% and reach a maximum of 46% in the case of CS4. Compared to the two line configuration (CS3), the scenario involving four generic marine farms (CS4) seems to offer a more effective coastal protection that can reduce at half the significant wave heights in some cases (ex: point N4).

Figure 7 is focused on a high energy summer event, being clearly highlighted the impact of the generic farms in the geographical space, even in the case of the scenario CS1. In this configuration, the shielding effect is more visible in the central part of the target area, especially in front of the Porto

Ferro inlet. The variations corresponding to the N-points indicate a similar pattern as the ones presented in Figure 6f, with the mention that in the case of N7 (*Hs* = 3.05 m), a wave farm located offshore (CS1) presents similar results with the ones corresponding to scenario CS2 (*Hs* = 3.08 m). The group points N4–N6 indicate lower *Hs* values in the case CS4, which drop from 3.5 m (no farm) to a minimum of 1.5 m.

Table 3. *Hs* variation (%) corresponding to the N-points, considering an energetic summer event (summer A). The results were compared with the no farm scenario.

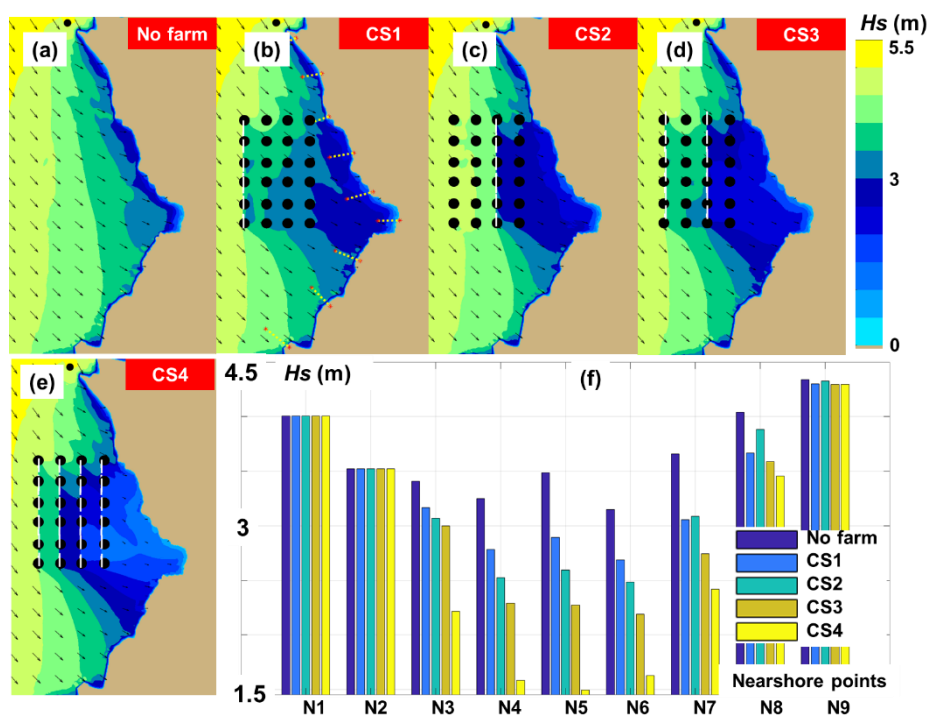| Scenario	Nearshore Points								
	N1	N2	N3	N4	N5	N6	N7	N8	N9
CS1	0	0.02	7.2	11	14	14	14	8.9	1.1
CS2	0	0.03	9	17	21	18	15	4.7	0.43
CS3	0	0.04	10	21	27	25	23	11	1.1
CS4	0	0.05	32	40	46	40	33	15	1.1

Figure 7. Influence of the generic marine farm taking into account a high energy summer event (case summer B as defined in Table 2). The results correspond to: (**a**–**e**) spatial variations of the wave conditions considering various scenarios; (**f**) distribution of the *Hs* values near the nearshore points N1–N9. The arrows field in the plot represent the wave direction.

Regarding the variations (in %), these values are included in Table 4. In general, the erosion processes were accentuated during the storm events, and by looking at these results, we notice that even a single generic farm located offshore (CS1) may reduce the wave heights, this being an expected result from the perspective of the coastal protection. For CS1 the *Hs* attenuation starts from 7% and reaches a maximum of 16% near the site N7, located south of Porto Ferro. The highest attenuation corresponds to CS4, around 50%, in the case of the reference points N4–N6.

Table 4. *Hs* variation (%) corresponding to the N-points, considering a high energy summer event (summer B). The results were compared with the no farm scenario.

Scenario	Nearshore Points								
	N1	**N2**	**N3**	**N4**	**N5**	**N6**	**N7**	**N8**	**N9**
CS1	0	0	7	14	17	15	16	9.3	0.99
CS2	0	0	9.9	22	26	21	16	3.9	0.39
CS3	0	0	12	30	35	30	25	11	1
CS4	0	0	35	51	57	48	34	14	1

In Figure 8 and Table 5, the wave coastal transformation is presented for a typical winter condition. Regardless of the scenario taken into account, there is a visible attenuation of the wave heights, this is the case of CS1 and CS2 when the values can decrease below a threshold of 1.5 m. The changes induced by CS3 and CS4 were more complex, being noticed the occurrence of some multiple wave fields. The highest influence is also between the generic lines., This can be considered a negative effect since the performances of some wave generators were influenced. The wave profiles along several reference lines were presented, each coastal sector indicating particular features. For the lines L3 and L6 there is a constant distribution of the *Hs* values until they collapse in the surf zone, being also noticed some bumps for the line L6 that can be associated to the local bathymetry (possible sand bars).
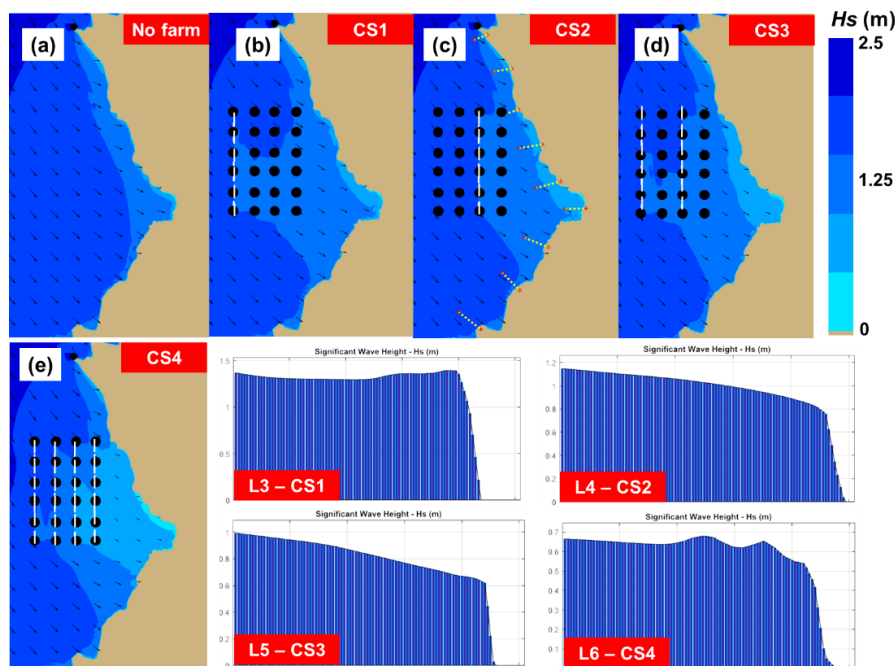

Figure 8. Influence of the generic marine farm taking into account an energetic winter event (case winter A as defined in Table 2). The results correspond to: (**a**–**e**) spatial variations of the wave conditions considering various scenarios. The *Hs* variation along the reference lines L3–L6 is also represented. The arrows field in the plot represent the wave direction.

Although the wave characteristics considered were a little higher than those corresponding to the Summer A situation, the differences were relatively close. Nevertheless, for the nearshore points N4–N7 the differences could increase up to 53% compared to only 46% for the summer scenario.

Table 5. *Hs* variation (%) corresponding to the N-points, considering an energetic winter event (winter A). The results were compared with the no farm scenario.

Scenario	Nearshore Points								
	N1	N2	N3	N4	N5	N6	N7	N8	N9
CS1	0	0	7.3	12	16	16	16	9.2	1.2
CS2	0	0	9.2	19	24	22	16	4.8	0.43
CS3	0	0	11	25	32	30	25	12	1.2
CS4	0	0	33	45	53	47	35	15	1.2

A similar analysis is presented in Figure 9, considering this time one of the highest wave events that may occur in this region, namely a winter storm. More significant results corresponded to the configuration CS4, which gradually attenuated the wave heights as they passed each generic line, in the context where almost 75% of the waves passed each line. A possible explanation would be that the incoming waves did not have enough space to regenerate, and this disruption was important for the coastal protection. Going closer to the shoreline, we noticed that wave heights were significantly reduced, indicating in general values below 4 m, as the the profile lines L3, L4 and L7 indicate.
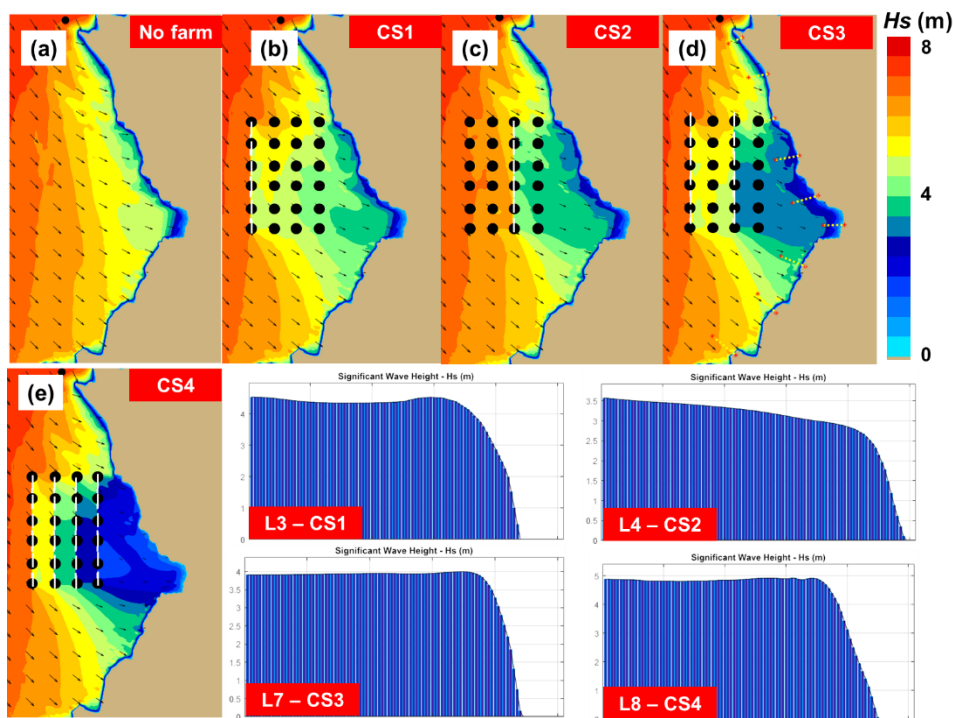

Figure 9. Influence of the generic marine farm taking into account an extreme winter event (case winter B as defined in Table 2). The results are reported for: (**a–e**) spatial variations of the wave conditions considering various scenarios. The *Hs* variations along the reference lines L3–L4 and L7–L8 are also represented. The arrows in the plots represent the wave direction.

The wave variations (*Hs* variation in %) are presented in Table 6. The current profiles along these lines did not change independently of the scenarios considered. However, some modifications were noticed in relationship with current velocity values, in the sense that they decreased from the no farm situation to CS4. The reference points N1–N9 (representing in fact the ends of the reference lines) indicated also these variations, which are presented in Tables 5 and 6. As we go from the scenario CS1 to CS4, various differences were noticed, namely: CS1 to CS2—2% to 9%; CS2 to CS3—2% to 10%; CS3 to CS4—4% to 23%; CS1 to CS3—5% to 18%; and CS1 to CS4—5% to 41%. Taking into account that at this moment there was no operational wind–wave farm, these differences

were just for guidance, since it is difficult to estimate what is the standard configuration of a wave farm (ex: how many lines; accepted distance to the shoreline, etc.).

Table 6. *Hs* variation (%) corresponding to the N-points, considering an extreme winter event (winter B). The results were compared with the no farm scenario.

Scenario	Nearshore Points								
	N1	**N2**	**N3**	**N4**	**N5**	**N6**	**N7**	**N8**	**N9**
CS1	0	0	7	15	17	6.7	17	9.1	0.78
CS2	0	0	10	23	26	10	15	3.2	0.31
CS3	0	0	12	31	35	18	25	10	0.79
CS4	0	0	35	53	58	38	33	14	0.83

Besides the significant wave heights, some other parameters were important for the coastal processes, this being the case for the wave direction presented in Figure 10. As expected, the results corresponding to the reference points N1, N2, and N9 did not indicate any variation, while for the group points N3–N5 there was a slight increase in this parameter. For the points N6–N8, the presence of a wave farm may have resulted in a decrease of the wave direction that could influence the erosion processes, especially for the reference point N6 (CS4).
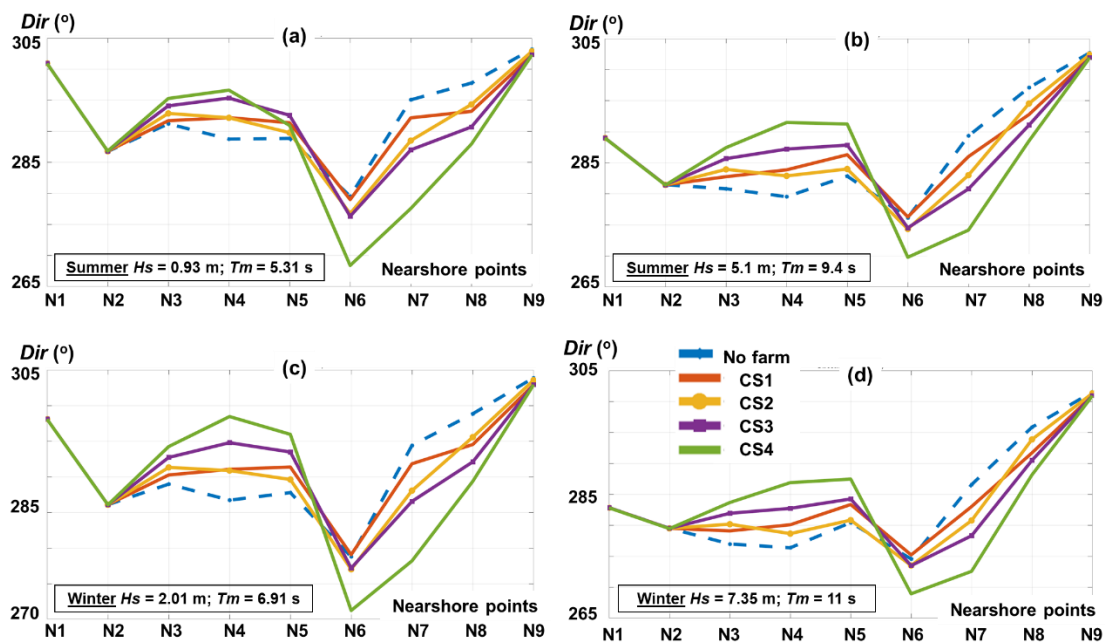

Figure 10. Wave directions (°) corresponding to the N-points for the four different scenarios considered.

It was noticed that for the summer A scenario (Figure 10a), the direction could shift from 279.5° to almost 268.4° (N6–CS4) or from 288.7° to 295.3 (N4–CS3). As we went south, the site N8 indicated a gradual variation from 297.8° (no farm) to 294.3° (CS2); 293.2° (CS1); 290.7° (CS3); or 287.9° (CS4). A similar pattern occurred for the summer B scenario, with the mention that the differences were higher. The direction could vary in the case of site N4 from 279.5° to 283.9° (CS1), reaching a maximum of 291.5° (CS4). For the site N6, the no farm and CS1 scenarios indicated similar values (276.3°). Similar variations were noticed in winter, when during a storm event the generic farm(s) could change the wave pattern from 276.4° to 286.9° (N4–CS4) or from 286.6° to 272.6° (N7–CS4). Since the wave direction is a crucial parameter in the development of the nearshore currents, the fact that the marine energy farm may produce significant changes in terms of wave direction may affect also the longshore current velocity [36,44]. That is why, although the waves lost energy in the

presence of the marine energy farm, in certain situations due to such changes in wave direction, the longshore current velocity could significantly increase down-wave from a marine energy farm. Such aspects are analyzed next.

3.3. Assessment of the Nearshore Currents

Nearshore currents represent another important element that influence the stability of a beach area, and therefore this section tackles this aspect. Figure 11 provides a first evaluation for the scenario summer A, where it was be noticed that for the reference lines the currents velocity was reduced, except line L6 (Porto Ferro inlet), where in fact the velocity was amplified for the scenarios CS1–CS3. For example, line L4 indicated a maximum velocity of 0.63 m/s (no farm) that was down to 0.47 m/s (CS4). Line L7 was defined by more significant variations, notably a decrease of the current velocity with almost 23% for CS1 and with a maximum of 41% for CS4. For the line L6, we expected an increase of 74% for CS1 and a decrease of 56% for the CS4, by taking as a reference the current value of 0.27 m/s (corresponding to the no farm situation).

Figure 12 is focused on a high energy summer event, showing in general a decrease of the velocity, except for the lines L3 and L4, where the cases CS1–CS3 indicated no significant impact. Line L6 presented significant variations, the values gradually decreasing from 1.35 m/s to 1.15 m/s (CS1); 0.88 m/s (CS2); 0.75 m/s (CS3); and 0.33 m/s (CS4). Line L7 indicated a maximum decrease, where the currents went from 2.04 m/s to almost 0.77 m/s in the presence of a CS4 configuration.
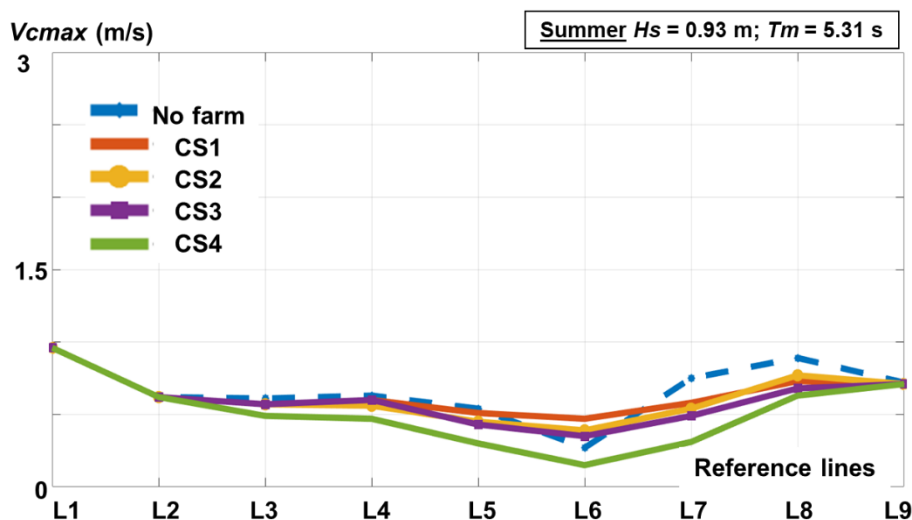

Figure 11. Maximum values of the nearshore current velocities along the reference lines considered. The results correspond to an energetic summer event (Summer A).

At this point, it has to be highlighted that, in some cases, the presence of a wave farm could induce various patterns, this being also noticed in Rusu and Onea [4]. According to these results (Figure 14, point NP1) the current velocity may increase in the presence of a farm defined by moderate absorption and decrease when we consider a high absorption scenario, which is comparable with CS4 used in our work.
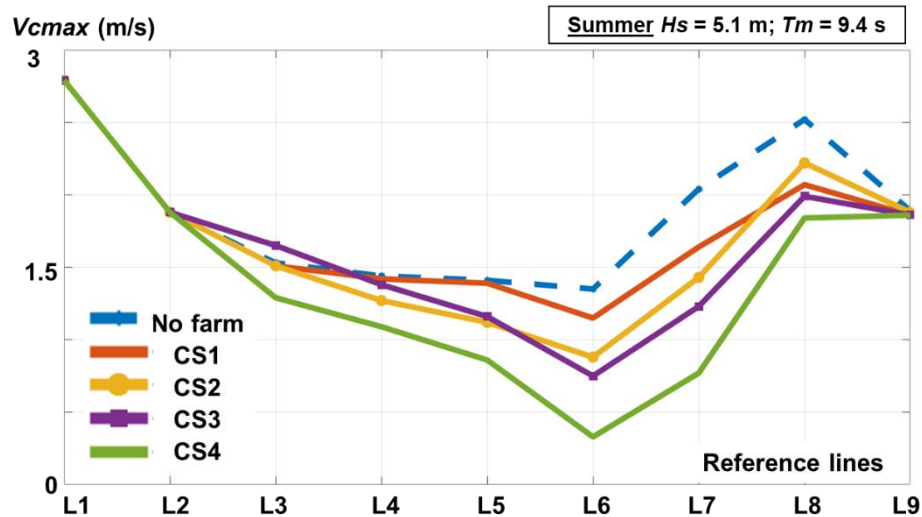
Figure 12. Maximum values of the nearshore current velocities along the reference lines considered. The results correspond to a high energy summer event (Summer B).

Going to the winter season, a similar pattern was noticed in Figure 13a, where the velocity oscillated between 0.17 m/s (L6–CS4) and 1.65 m/s (line L1). As the waves entered in the surf area they finally reached their end life and broke under one of the following forms: spilling, plunging, collapsing, or surging. From all these, only the spilling waves interact with the seabed, and therefore would be able to push more sediments into the surf zone [45]. In Figures 13b and 13c, the balance between the breaking waves is presented for two reference lines (L3 and L6), which is divided between spilling and plunging. In the case of line CS4, the plunging waves became dominant (100%) as we went from no farm to CS4, but in the case of line L6, the spilling waves became dominant when a CS3 or CS4 configuration was considered. In a similar way, Figure 14 presents a high energy winter event that may occur in this region.
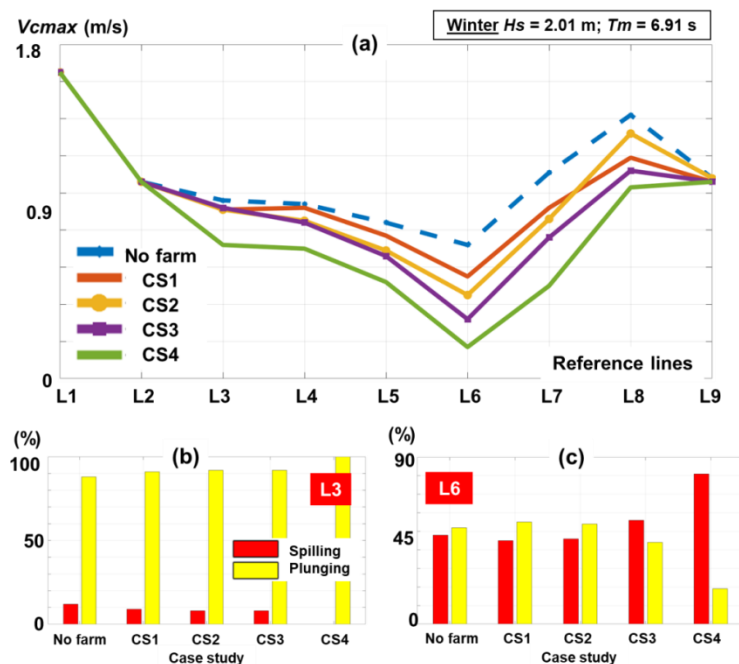

Figure 13. Evaluation of the nearshore processes considering an energetic winter event (winter A), where: (**a**) maximum nearshore current velocities (in m/s) along the reference lines; (**b**) and (**c**) balance between the wave spilling and plunging along the lines L3 and L6, in percentage.
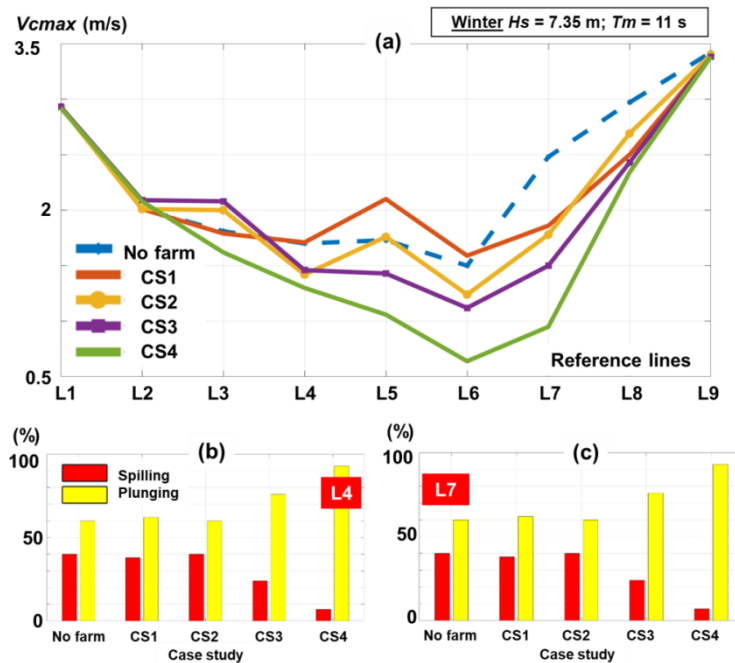
Figure 14. Evaluation of the nearshore processes considering a high energy winter event (winter B), where: (**a**) maximum nearshore current velocities (in m/s) along the reference lines; (**b**) and (**c**) balance between the wave spilling and plunging along the lines L4 and L7, in percentage.

Compared to the previous scenarios, for line L5 CS1 and CS2 would have little effect or would accelerate the current velocity, while for the L3 only CS4 would reduce the current velocity from 1.81 m/s to almost 1.62 m/s. In terms of the breaking waves, the reference lines L4 and L7 indicated the plunging waves as being dominant, the impact of the configurations CS3 and CS4 being to accentuate the occurrences of the plunging waves.

4. Conclusions

By extracting the energy from waves through a marine farm, it possible to attenuate their action at the shoreline level, an aspect that is directly related to coastal erosion [46–49]. In order to develop such complex projects, one way will be to use the infrastructure of offshore wind farms located in coastal areas, affected by the erosion problems associated to the wave action. Motivated by the fact that there is a problem with the coastal erosion in the Mediterranean islands, and that the north-western region is defined by more consistent wave resources, in the present work we evaluate the expected nearshore impact of a generic marine farm that would be implemented near the Porto Ferro inlet (northwest Sardinia)

At this point, it is important to mention that excepting the work of Onea and Rusu [42], the problem of coastal impact of a marine farm located in the Mediterranean Sea was not taken into consideration yet, and therefore there is room for improvement. Compared to the previous study, the wave dataset was extended from 20 years to 40 years and new scenarios were taken into account, while as an element of novelty, the variations of the nearshore currents were also discussed. In a similar way, a generic farm was considered in Rusu and Onea [4] in order to assess the impact of a project near the Portuguese nearshore (Pinheiro da Cruz area south of Lisbon). Several distances from the shore were considered, while the WEC absorption was set to 20% (moderate) and 40% (high), respectively. In the case of the current velocity, various patterns were noticed in the presence of the farm (increase or decrease of the velocity), these variations being related more to the characteristics of the breaking waves (e.g., direction). In Zanopol et al. [50] a generic wave farm located in front of the Danube Delta was considered for simulation, by taking into account an absorption interval that started from 0% and ended with 100%. As expected, in this case the wave reduction was directly related to the absorption property, and also noticed were various patterns in

terms of the current velocity. However, a complete discussion on this topic is difficult to carry out, since at this moment there is no operational wave farm and therefore most of the existing studies are focused on theoretical case studies. More than this, each geographical area is defined by particular characteristics from which we can mention the bathymetry, the orientation of the shoreline, or the severity of the wave conditions [51–53].

Three research questions were used to guide the present work and these are the findings:

a) Wave conditions: The north-western part of the Mediterranean Sea is characterized by more important wave resources and in particular the western part of Sardinia is more energetic.

b) Impact on the local wave resources: The presence of a wave farm (CS3 and CS4—winter/line L6), can shift the breaking patterns of the waves from plunging to spilling, an aspect that can be considered beneficial for a beach sector, since more sediments will be transported to the surf area.

c) Variations of the nearshore currents: In general, the current velocity decreases in the presence of the WEC lines, with an exception for the scenario summer A (line L6, Porto Ferro inlet).

Finally, it has to be highlighted that for a remote island area, a marine renewable farm represents a double-win, since it is possible to protect some important touristic areas and to make a step forward in the consolidation of the local electricity market that in most of the cases relies on fossil fuel imports.

Abbreviations

σ	relative frequency
θ	wave direction
$\vec{V}$	velocity of the ambient current
$\vec{c}_g$	relative group velocity of waves
$c_\sigma = \dot{\sigma}$	wave propagation velocity in the frequency space
$c_\theta = \dot{\theta}$	wave propagation velocity in the directional space
τ_y^r	longshore directed radiation stress
τ_y^b	wave averaged bottom stress
τ_y^w	the long-shore wind stress
ADCP	acoustic Doppler current profiler
CS	scenario
Dir	mean wave direction
ECMWF	European Center for Medium-Range Weather Forecasts
Hs	significant wave height
ISSM	interface for SWAN and surf models
S	source and sink terms
SWAN	simulating waves nearshore
Tm	mean wave period

References

1. Astariz, S.; Iglesias, G. Output power smoothing and reduced downtime period by combined wind and wave energy farms. *Energy* **2016**, *97*, 69–81.
2. Fernandez, G.V.; Balitsky, P.; Stratigaki, V.; Troch, P. Coupling Methodology for Studying the Far Field Effects of Wave Energy Converter Arrays over a Varying Bathymetry. *Energies* **2018**, *11*, 2899.
3. Folley, M.; Babarit, A.; Child, B.; Forehand, D.; O'Boyle, L.; Silverthorne, K.; Spinneken, J.; Stratigaki, V.; Troch, P. *A Review of Numerical Modelling of Wave Energy Converter Arrays*; American Society Mechanical Engineers: New York, NY, USA, 2013; ISBN 978-0-7918-4494-6.
4. Rusu, E.; Onea, F. Study on the influence of the distance to shore for a wave energy farm operating in the central part of the Portuguese nearshore. *Energy Convers. Manag.* **2016**, *114*, 209–223.
5. Onea, F.; Rusu, E. The expected efficiency and coastal impact of a hybrid energy farm operating in the Portuguese nearshore. *Energy* **2016**, *97*, 411–423.
6. Diaconu, S.; Rusu, E. The Environmental Impact of a Wave Dragon Array Operating in the Black Sea. *Sci. World J.* **2013**, *2013*, 498013.
7. Bento, A.R.; Rusu, E.; Martinho, P.; Soares, C.G. Assessment of the changes induced by a wave energy farm in the nearshore wave conditions. *Comput. Geosci.* **2014**, *71*, 50–61.
8. Tomey-Bozo, N.; Babarit, A.; Murphy, J.; Stratigaki, V.; Troch, P.; Lewis, T.; Thomas, G. Wake effect assessment of a flap type wave energy converter farm under realistic environmental conditions by using a numerical coupling methodology. *Coast. Eng.* **2019**, *143*, 96–112.
9. Fadaeenejad, M.; Shamsipour, R.; Rokni, S.; Gomes, C. New approaches in harnessing wave energy: With special attention to small islands. *Renew. Sustain. Energy Rev.* **2014**, *29*, 345–354.
10. Veigas, M.; Carballo, R.; Iglesias, G. Wave and offshore wind energy on an island. *Energy Sustain. Dev.* **2014**, *22*, 57–65.
11. Rusu, E.; Onea, F. An assessment of the wind and wave power potential in the island environment. *Energy* **2019**, *175*, 830–846.
12. Liberti, L.; Carillo, A.; Sannino, G. Wave energy resource assessment in the Mediterranean, the Italian perspective. *Renew. Energy* **2013**, *50*, 938–949.
13. Franzitta, V.; Curto, D. Sustainability of the Renewable Energy Extraction Close to the Mediterranean Islands. *Energies* **2017**, *10*, 283.
14. Ayat, B. Wave power atlas of Eastern Mediterranean and Aegean Seas. *Energy* **2013**, *54*, 251–262.
15. Cavaleri, L. The wind and wave atlas of the Mediterranean Sea—The calibration phase. *Adv. Geosci.* **2005**, *2*, 255–257.
16. Soukissian, T.H.; Denaxa, D.; Karathanasi, F.; Prospathopoulos, A.; Sarantakos, K.; Iona, A.; Georgantas, K.; Mavrakos, S. Marine Renewable Energy in the Mediterranean Sea: Status and Perspectives. *Energies* **2017**, *10*, 1512.
17. Rusu, L.; Onea, F.; Deleanu, L.; Georgescu, C. Evaluation of the wind energy potential along the Mediterranean Sea coasts. *Energy Explor. Exploit.* **2016**, *34*, 766–792.
18. Lavidas, G.; Venugopal, V. Energy Production Benefits by Wind and Wave Energies for the Autonomous System of Crete. *Energies* **2018**, *11*, 2741.
19. Vannucchi, V.; Cappietti, L. Wave Energy Assessment and Performance Estimation of State of the Art Wave Energy Converters in Italian Hotspots. *Sustainability* **2016**, *8*, 1300.
20. Iuppa, C.; Cavallaro, L.; Vicinanza, D.; Foti, E. Investigation of suitable sites for Wave Energy Converters around Sicily (Italy). *Ocean Sci. Discuss.* **2015**, *12*, 315–354.
21. Khalifehei, K.; Azizyan, G.; Gualtieri, C. Analyzing the Performance of Wave-Energy Generator Systems (SSG) for the Southern Coasts of Iran, in the Persian Gulf and Oman Sea. *Energies* **2018**, *11*, 3209.
22. McGlashan, D.J. Corine: Coastal Erosion by R.E. Quelennec, European Commission, 170p, 88 Maps, £12.50 (pbk). Available online: https://onlinelibrary.wiley.com/doi/abs/10.1002/%28SICI%291099-1719%28200005%298%3A2%3C122%3A %3AAID-SD136%3E3.0.CO%3B2-%23 (accessed on 30 August 2019).
23. https://www.bbc.com/news/world-europe-41031029 BBC News: London, UK, 2017, (accessed on 30 August 2019).
24. De Muro, S.; Di Martino, G.; Perilli, A.; De Falco, G.; Budillon, F.; Conforti, A.; Innangi, S.; Tonielli, R.; Simeone, S. Sandy beaches characterization and management of coastal erosion on western Sardinia island (Mediterranean Sea). *J. Coast. Res.* **2014**, *70*, 395–400.

25. Ballesteros, C.; Jiménez, J.A.; Valdemoro, H.I.; Bosom, E. Erosion consequences on beach functions along the Maresme coast (NW Mediterranean, Spain). *Nat. Hazards* **2018**, *90*, 173–195.

26. Enríquez, A.R.; Marcos, M.; Falqués, A.; Roelvink, D. Assessing Beach and Dune Erosion and Vulnerability Under Sea Level Rise: A Case Study in the Mediterranean Sea. *Front. Mar. Sci.* **2019**, *6*, 4.

27. Reimann, L.; Vafeidis, A.T.; Brown, S.; Hinkel, J.; Tol, R.S.J. Mediterranean UNESCO World Heritage at risk from coastal flooding and erosion due to sea-level rise. *Nat. Commun.* **2018**, *9*, 4161.

28. Monioudi, I.N.; Velegrakis, A.F.; Chatzipavlis, A.E.; Rigos, A.; Karambas, T.; Vousdoukas, M.I.; Hasiotis, T.; Koukourouvli, N.; Peduzzi, P.; Manoutsoglou, E.; et al. Assessment of island beach erosion due to sea level rise: The case of the Aegean archipelago (Eastern Mediterranean). *Nat. Hazards Earth Syst. Sci.* **2017**, *17*, 449–466.

29. Ciortan, S.; Onea, F.; Rusu, E. Assessment of the potential for developing combined wind-wave projects in the European nearshore. *Energy Environ.* **2017**, *28*, 580–597.

30. Osti, G. The uncertain games of energy transition in the island of Sardinia (Italy). *J. Clean. Prod.* **2018**, *205*, 681–689.

31. Andreucci, S.; Clemmensen, L.B.; Murray, A.S.; Pascucci, V. Middle to late Pleistocene coastal deposits of Alghero, northwest Sardinia (Italy): Chronology and evolution. *Quat. Int.* **2010**, *222*, 3–16.

32. De Rosa, B.; Cultrone, G. Assessment of two clayey materials from northwest Sardinia (Alghero district, Italy) with a view to their extraction and use in traditional brick production. *Appl. Clay Sci.* **2014**, *88*, 100–110.

33. Dee, D. ERA-Interim. Available online: https://www.ecmwf.int/en/forecasts/datasets/archive-datasets/reanalysis-datasets/era-interim (accessed on 15 May 2018).

34. Vicinanza, D.; Contestabile, P.; Ferrante, V. Wave energy potential in the north-west of Sardinia (Italy). *Renew. Energy* **2013**, *50*, 506–521.

35. Rusu, E.; Conley, D.; Ferreira-Coelho, E. A hybrid framework for predicting waves and longshore currents. *J. Mar. Syst.* **2008**, *69*, 59–73.

36. Rusu, E.; Macuta, S. Numerical modelling of longshore currents in marine environment. *Environ. Eng. Manag. J.* **2009**, *8*, 147–151.

37. Rusu, E.; Soares, C.G. Validation of Two Wave and Nearshore Current Models. *J. Waterw. Port Coast. Ocean Eng.* **2010**, *136*, 27–45.

38. Gonçalves, M.; Rusu, E.; Soares, C.G. Evaluation of Two Spectral Wave Models in Coastal Areas. *J. Coast. Res.* **2015**, *300*, 326–339.

39. Booij, N.; Ris, R.C.; Holthuijsen, L.H. A third-generation wave model for coastal regions: Model description and validation. *J. Geophys. Res. Space Phys.* **1999**, *104*, 7649–7666.

40. Mettlach, T.R.; Earle, M.D.; Hsu, Y.L. *Software Design Document for the Navy Standard Surf Model Version 3.2*; Defense Technical Information Center: Fort Belvoir, VA, USA, 2002.

41. Power Plants: Kentish Flats—Vattenfall. Available online: https://powerplants.vattenfall.com/en/kentish-flats (accessed on 10 September 2019).

42. Onea, F.; Rusu, L. Coastal impact of a hybrid marine farm operating close to the Sardinia Island. In Proceedings of the OCEANS 2015, Genoa, Italy, 18–21 May 2015; pp. 1–7.

43. Stokes, C.; Conley, D.C. Modelling Offshore Wave farms for Coastal Process Impact Assessment: Waves, Beach Morphology, and Water Users. *Energies* **2018**, *11*, 2517.

44. Rusu, E.; Soares, C.G. Wave modelling at the entrance of ports. *Ocean Eng.* **2011**, *38*, 2089–2109.

45. NOAA Ocean Explorer: Education—Multimedia Discovery Missions: Lesson 9—Ocean Waves: Activities: Breaking Waves. Available online: https://oceanexplorer.noaa.gov/edu/learning/9_ocean_waves/activities/breaking_waves.html (accessed on 12 September 2019).

46. Zanopol, A.T.; Onea, F.; Rusu, E. Evaluation of the Coastal Influence of a Generic Wave Farm Operating in the Romanian Nearshore. *J. Environ. Prot. Ecol.* **2014**, *15*, 597–605.

47. Rusu, E.; Soares, C.G. Coastal impact induced by a Pelamis wave farm operating in the Portuguese nearshore. *Renew. Energy* **2013**, *58*, 34–49.

48. Koftis, T.; Prinos, P.; Stratigaki, V. Wave damping over artificial Posidonia oceanica meadow: A large-scale experimental study. *Coast. Eng.* **2013**, *73*, 71–83.

49. Balitsky, P.; Quartier, N.; Fernandez, G.V.; Stratigaki, V.; Troch, P. Analyzing the Near-Field Effects and the Power Production of an Array of Heaving Cylindrical WECs and OSWECs Using a Coupled Hydrodynamic-PTO Model. *Energies* **2018**, *11*, 3489.

50. Zanopol, A.T.; Onea, F.; Rusu, E. Coastal impact assessment of a generic wave farm operating in the Romanian nearshore. *Energy* **2014**, *72*, 652–670.

51. Rodriguez-Delgado, C.; Bergillos, R.J.; Iglesias, G. Dual wave farms for energy production and coastal protection under sea level rise. *J. Clean. Prod.* **2019**, *222*, 364–372.

52. Rodriguez-Delgado, C.; Bergillos, R.J.; Iglesias, G. Dual wave farms and coastline dynamics: The role of inter-device spacing. *Sci. Total Environ.* **2019**, *646*, 1241–1252.

53. Bergillos, R.J.; Lopez-Ruiz, A.; Medina-Lopez, E.; Monino, A.; Ortega-Sanchez, M. The role of wave energy converter farms on coastal protection in eroding deltas, Guadalfeo, southern Spain. *J. Clean. Prod*. **2018**, *171*, 356–367.